Fabrication of F-Inverted Compact Antenna Using a 3D Printer

Laura Audino and Adrian Caldow
Defence Science and Technology Organisation
PO Box 1500, Edinburgh, S.A. 5111

***Abstract*—The fabrication of an electrically small 916 MHz F-Inverted Compact Antenna (FICA) suitable for use in Wireless Sensor Network (WSN) applications is reported. The design is constructed using a consumer quality 3D desktop printer to produce a dielectric former onto which a wire helical element is wound. The use of a printed former eliminates several variances that arise when the antenna is entirely constructed by hand, leading to a more repeatable and robust fabrication approach.**

***Index Terms*—Additive manufacturing, 3D printing, electrically small antennas, wireless sensor networks.**

I. Introduction

The development of Electrically Small Antennas (ESAs) has long been a topic of interest to researchers [1]-[2], with modern efforts focusing on Personal Communication Systems (PCS) [3] and Wireless Sensor Networks (WSN) [4]-[5]. The increased availability of low power chip scale transceivers and improvements in battery technology has meant that antenna size has become a dominant factor limiting the miniaturisation of WSN nodes. It is documented that effectively utilising the total available volume results in increased performance for a given dimension [2]. To achieve this, some designers [4] have adapted planar construction techniques by joining multiple planar structures to form a 3D antenna. More elaborate techniques have involved the printing of conductive inks directly onto spherical surfaces [6].

The recent widespread availability of low cost additive manufacturing technology, more commonly known as 3D printing, has created a new option for the fabrication of electrically small 3D antennas. No longer do designers need to focus on structures that can be easily manufactured using planar fabrication techniques such as etching and PCB milling. 3D printing allows the rapid realisation of complex 3D objects with arbitrary geometry by building the object layer by layer using a range of materials, including plastics and metals. Although the full potential of applying 3D printing for complex antenna designs has yet to be fully realised, the technology has already been applied in numerous antenna designs. These include, printing a Ku band horn antenna using a metal 3D printer [7] and fabricating a spherical wire antenna by printing a plastic structure and then coating the surface with a conductive paint [8].

In this paper we explore a hybrid approach that utilises a low cost Fused Deposition Modelling (FDM) 3D printer to aid the construction of a F-Inverted Compact Antenna (FICA), whilst still incorporating traditional wire and printed circuit board (PCB) materials. The FICA was specifically developed as an ultra compact antenna suitable for WSN, resulting in a very limited ground plane size [5]. As is typical for most ESAs, the FICA has a very narrow bandwidth, which is not an issue for a narrow band WSN provided the design is robust to detuning in its operational environment. The intent of this work is to develop a robust and repeatable construction technique to quickly fabricate a FICA to closely match the desired simulated performance.

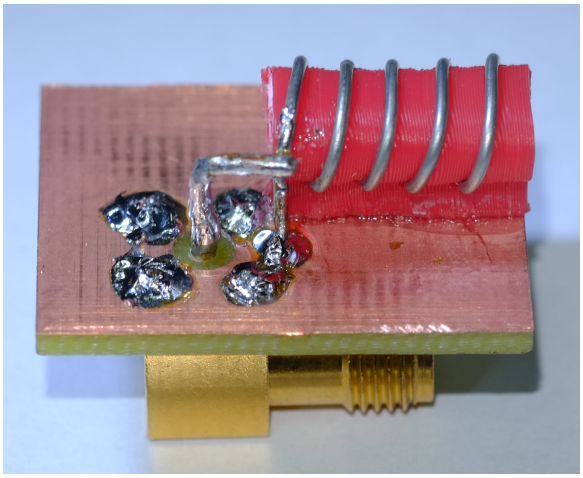

Fig. 1. FICA Design

II. FICA Antenna Design and Fabrication

A. FICA Design

The FICA structure consists of a shorted helical coil running parallel to a ground plane and a vertical feed pin that taps onto the helical coil in a similar fashion to an inverted F antenna (IFA) as shown in Fig. 1. The size of a IFA can be reduced by increasing the effective current path length, through geometry changes such as meandering and slots, or by dielectric loading. With the FICA, the length of the horizontal arm of the IFA is shortened by creating a helical coil, which also acts to add inductance to counter the capacitance inherent in ESAs. This allows for the FICA to be matched to 50Ω without the additional loss caused by lumped components in a matching circuit [9]. The overall size can be further reduced by winding the helical coil around a former to provide dielectric loading.

The currents on the vertical feed and short pins are in phase, similar to a IFA, which reinforces the vertical component of radiation. The distance of the helical coil above the ground plane is much smaller than a wavelength, so radiation

 Copyright (C) 2015 IEICE

contributions from the current flowing in the horizontal coil and its image cancel in the far field. This leads to the vertically polarized E-field (E_θ) being the dominant radiation component, with omni-directional radiation in the azimuth plane. The length of the wire in the coil plus the feed pin height is approximately a quarter-wavelength and the resonant frequency can be tuned by shortening the coil, similar to a IFA.

For consistency with [5], the antenna was designed using ANSYS HFSS V15 to operate at 916 MHz using a 20 mm x 25 mm ground plane, total height of 8 mm, helical pitch of 2.5 mm and a helical to ground separation of 3 mm. The HFSS model is shown in Fig. 2. Simulations were conducted to optimise the number of helix turns, major and minor radii of the elliptical helix, feed pin and short spacing, and feed pin height. The number of turns and the radius of the helix affect the length of the helix, which directly relates to the resonant frequency, and the feed pin height and spacing determine the match.

The FICA's high Q places a high importance on the fabrication tolerances and robustness to prevent detuning. By printing a dimensionally accurate Acrylonitrile Butadiene Sytrene (ABS) former, several variances that arise when the antenna is entirely constructed by hand are eliminated, leading to a more repeatable and robust fabrication process. Initial FICA prototypes wound free hand around dielectric elliptical cylinder formers were found to easily detune if the helical pitch or height above the ground plane changed. To address this issue, the use of a 3D printed elliptical cylinder former with integrated winding groove and ground spacing block was developed as shown in Fig. 3. The accuracy of the printed 3D former allows for the helical to be easily fabricated to match the simulation model and provides a robust construction technique that can't easily detune once the fabrication and measurement process is complete.

Due to the dielectric loading provided by the ABS former, which decreases the resonant frequency by 13%, accurate modelling of the dielectric constant (ϵ_r) and loss tangent ($\tan\delta$) of the ABS is critical for close agreement between simulation and measurement. For ABS, there are a wide range of values reported in the literature including specific materials related to FDM 3D printing [10]-[11]. The work detailed in [11], utilised a Makerbot Replicator FDM printer to construct an ABS multilayer transmission line and achieved a good match between measurement and simulation using ϵ_r = 2.7 and $\tan\delta$ = 0.01. Based on these results, these ABS properties were used for the FICA simulations.

B. Fabrication

The 3D CAD model of the former, as shown in Fig. 3, was exported from HFSS and printed using a Makerbot Replicator 2X, shown in Fig. 4, with Makerbot ABS filament using a 90% infill and 0.15 mm layer height. The extruder and build plate temperatures were 230°C and 130°C respectively. By printing with the helical axis aligned vertically, an accurate helical former with integrated helical wire groove could be achieved without the need for any support structures. Although holes for the helical winding are included in the ground spacing block, it was necessary to widen these using a drill in a pin

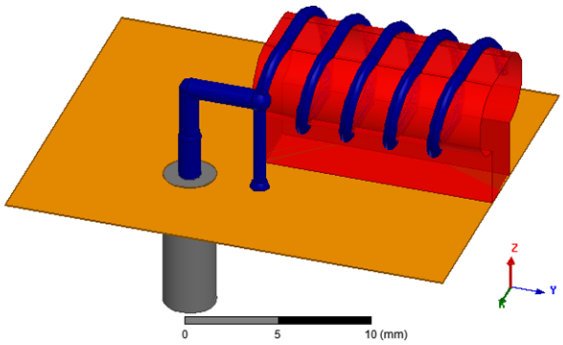

Fig. 2. FICA HFSS model.

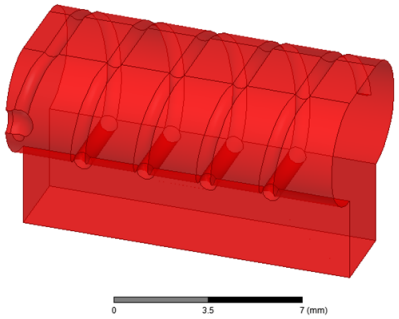

Fig. 3. CAD Former model.

vice due to the holes partially closing over during the printing process. Once the former has been printed, the helical coil was created by winding a 0.7 mm tinned copper wire around the former, making sure the wire was wound tightly into the printed groove. The completed helical assembly was then glued to the top surface of single sided FR-4 ground plane, and the shorting pin soldered to ground, ensuring the correct separation between the helical feed and shorting pins. The final step was to install a SMA connector to feed the FICA, through pre-drilled holes in the ground plane, and solder the feed tap point at the correct height from the ground plane.

III. Simulations and Measurements

A. Return Loss

The simulated and measured return loss for the presented FICA design is shown in Fig. 5. The plot shows reasonable agreement between measured and simulated results, with a 10 dB return loss bandwidth of 1.9% and 1.1% respectively. To suppress any radiation caused by currents induced in the feed cables, multiple ferrite chokes were placed on the feed cable in close proximity to the SMA connector. The fact that the simulated bandwidth is less than the measured bandwidth is consistent with results from [5], although the difference between them is greater, possibly due to increased losses associated with the dielectric loading. Simulations undertaken to analyse the impact of errors in the modelled ϵ_r and $\tan\delta$ showed that the resonant frequency is dependent on ϵ_r and the input match is dependent on $\tan\delta$ and the feed pin tap height.

To assess the consistency of the fabrication process, three

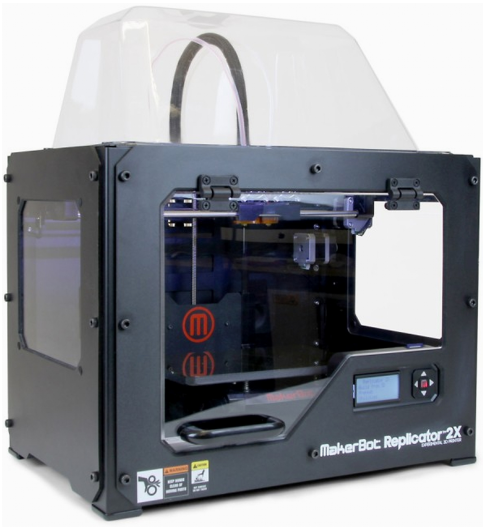

Fig. 4. Makerbot Replicator 2X.

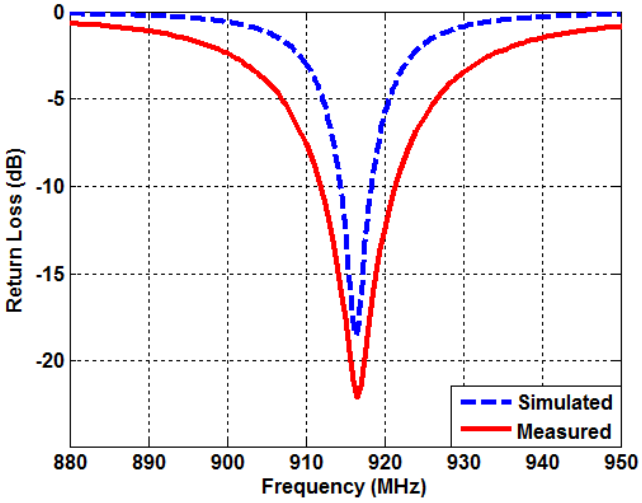

Fig. 5. Simulated and measured return loss of the FICA with ABS former.

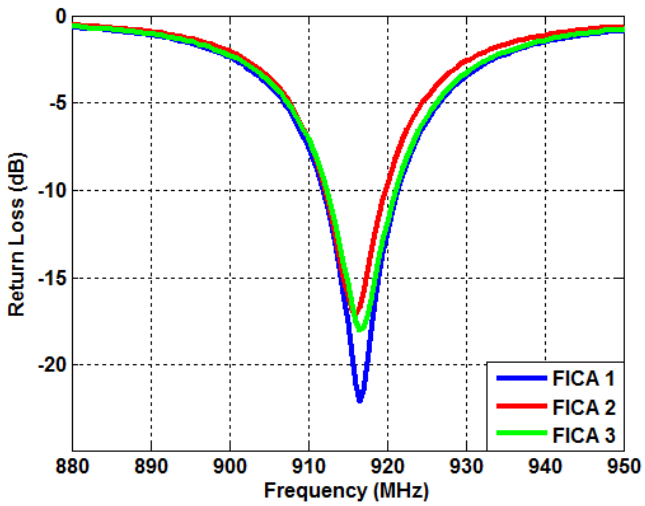

Fig. 6. Measured return loss of three separate identical FICAs.

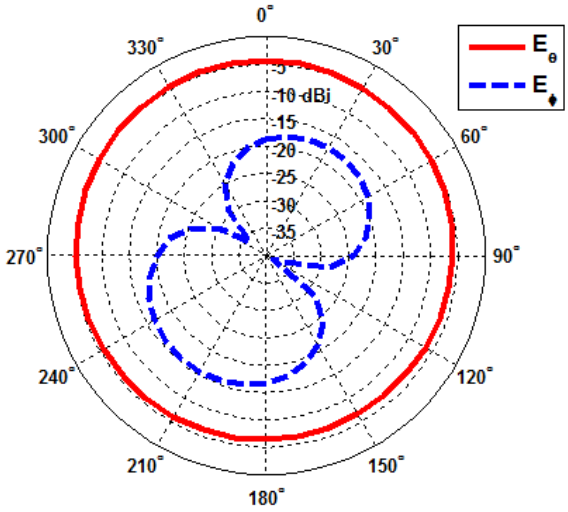

Fig. 7. Measured radiation pattern at 916 MHz for x-y plane.

separate but identical FICAs were constructed on formers printed using the same 3D model. The measured return losses for the constructed antennas are shown in Fig. 6. The results show close agreement between the three samples, without the need for secondary tuning to achieve the desired match and resonant frequency. This demonstrates that the fabrication technique would be suitable for construction of a large number of identical sensor nodes, typically required for deployment of a WSN.

B. Radiation Pattern Performance

To verify performance, radiation patterns for the fabricated FICA were measured in an ETS-Lindgren AMS-8050 anechoic chamber. The results are shown in Fig. 7-9 at x-y, y-z, and x-z planes for co-polarization (E_θ) and cross-polarization (E_ϕ). As simulations showed, the dominate radiation component is the vertically polarized E-field (E_θ). In the azimuth plane (x-y plane), the radiation pattern is omnidirectional, with a gain of -4.3 dBi. In the elevation planes (x-z and y-z), the peak gain is -4.0 dBi and the patterns are similar to a monopole, with nulls above and below the ground plane, and a slight asymmetry thought to be due to the offset on the ground plane. This measured gain is less than other ESAs, however the antenna volume is significantly smaller. With a larger ground plane, the gain of the FICA increases as expected.

IV. Conclusion

This work demonstrates that a hybrid approach which combines 3D printing with more traditional wire and PCB materials can produce a low cost and robust fabrication process for 3D ESAs. The precise geometries created by 3D printing simplify the fabrication of complex antenna structures, ensuring the realised design closely matches the intended performance. Future work will explore verifying specific material properties of MakerBot FDM ABS plastics that are critical for accurate dielectric modelling.

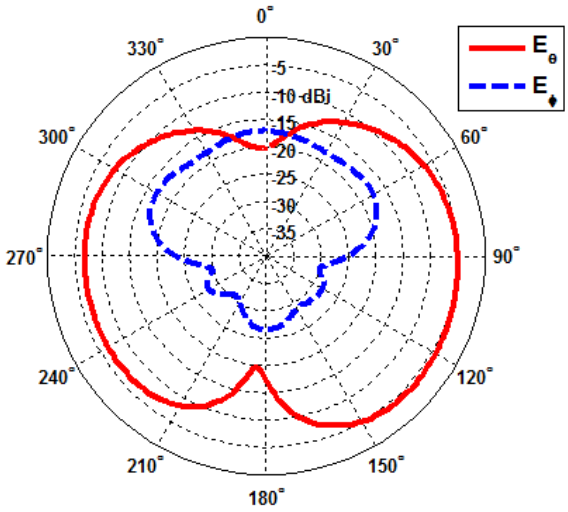

Fig. 8. Measured radiation pattern at 916 MHz for x-z plane.

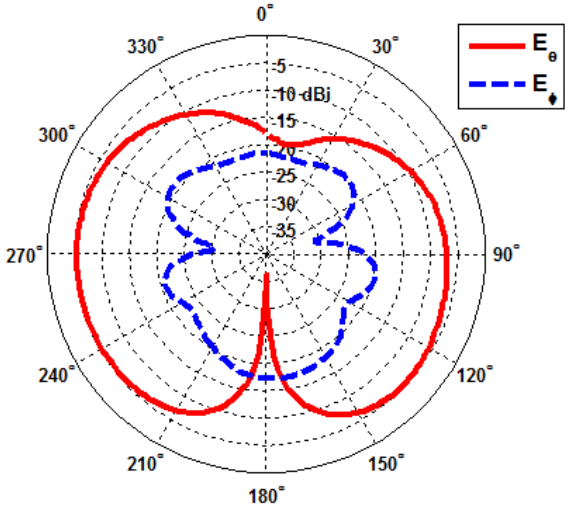

Fig. 9. Measured radiation pattern at 916 MHz for y-z plane.

REFERENCES

[1] L. Chu, "Physical limitations of omni-directional antennas," *Journal Appl. Phys.*, vol. 19, no. 12, pp. 1163-1175, 1948.

[2] H. Wheeler, "Fundamental limitations of small antennas," *IRE*, vol. 35, no. 12, pp. 1479-1484, Dec. 1947.

[3] A. Shrivervik *et al.*, "PCS antenna design: The challenge of minaturization," *IEEE Antennas Propag. Mag.*,vol. 43, no. 4, pp. 12-27, 2001.

[4] I. Nassar and T. Weller, "Development of novel 3-D cube antennas for compact wireless sensor nodes," *IEEE Trans. Antennas Propag.*, vol. 60, no. 2, pp. 1059-1065, Feb. 2012.

[5] B. Yang *et al.*, "916 MHz F-inverted compact antenna (FICA) for highly integrated transceivers,"*IEEE Antennas Wireless Propag. Lett.*, vol. 8, pp. 181-184, 2009.

[6] J. Adams *et al.*, "Comparison of spherical antennas fabricated via conformal printing: Helix, Meanderline, and Hybrid Designs," *IEEE Antennas Wireless Propag. Lett.*, vol. 10, pp. 1425-1428, 2011.

[7] C. Garcia *et al.*, "Effects of extreme surface roughness on 3D printed horn antenna," *IEEE Electronics Letters*, vol. 49, no. 12, pp. 734-736, June 2013.

[8] O. Kim, "3D printing electrically small spherical antennas," in *in Proc. IEEE Antennas Propag. Soc. Int. Symp.*, Orlando, USA, Jul. 713, 2013, pp. 776-777.

[9] K. Fujimoto and H. Morishita, "Principles and techniques for making antennas small," in *Modern Small Antennas*, Cambridge, UK, Cambridge University Press, 2013.

[10] P. Deffenbaugh, "3D Printed electromagnetic transmission and electronic structures fabricated on a single platform using advanced process integration techniques," Ph.D. dissertation, Dept. Elect. Comp. Eng., Univ. Texas, El Paso, Tx, 2014.

[11] M. Liang *et al.*, "3D Printed multilayer microstrip line structure with vertical transition toward integrated system," *Int. Microwave Symp.*, Phoenix, USA, May 17-22, 2015